Kidney International, Vol. 65 (2004), pp. 2091–2107

Losartan modulation on NOS isoforms and COX-2 expression in early renal fibrogenesis in unilateral obstruction

WALTER MANUCHA, LILIANA OLIVEROS, LILIANA CARRIZO, ALICIA SELTZER, and PATRICIA VALLÉS

Cátedra de Fisiopatología, Facultad de Ciencias Médicas, Universidad Nacional de Cuyo, Centro Universitario, Mendoza, Argentina; Cátedra de Química Biológica, Facultad de Química, Bioquímica y Farmacia, Universidad Nacional de San Luis, San Luis, Argentina; Cátedra de Fisiología Patólogica, Facultad de Ciencias Médicas, Universidad Nacional de Cuyo, Mendoza, Argentina; Consejo Nacional de Investigaciones Científicas y Tecnológicas; and Cátedra de Fisiología Patológica, Facultad de Ciencias Médicas, Universidad Nacional de Cuyo, Mendoza, Argentina

Losartan modulation on NOS isoforms and COX-2 expression in early renal fibrogenesis in unilateral obstruction.

Background. Angiotensin II plays a central role in the initiation of renal fibrogenesis at a very early stage leading to a rapid progression in unilateral ureteral obstruction (UUO). We examined the effect of an angiotensin II receptor inhibitor (AT_1) losartan, independent from its effects on blood pressure, on nitric oxide synthase (NOS) isoforms and cyclooxygenase-2 (COX-2) expression and the significance of this interaction on interstitial fibrosis in UUO.

Methods. Rats underwent UUO for 24 hours or control sham operation after been treated with losartan in the drinking water at 10 mg/kg/day for 15 days. AT_1 receptor binding and distribution was determined by in situ autoradiographic study. Renal fibrosis was evaluated through the relative volume of the tubulointerstitium (Vv) measured by an image analyzer, and transforming growth factor-β (TGF-β) at mRNA levels. NOS activity, expression of NOS isoforms by reverse transcription-polymerase chain reaction (RT-PCR) assay and COX-2 protein expression, were determined.

Results. After administration of a nonhypotensive dose of losartan prevention of renal fibrogenesis was demonstrated in obstructed kidneys by means of Vv values and TGF-β mRNA expression near controls. Decreased AT_1 receptor binding density was observed in cortex and inner stripe of the outer medulla of nontreated obstructed kidney compared to control, whereas no differences were observed in ipsilateral UUO related to obstructed kidney–treated group.

The increased inducible NOS (iNOS) activity and expression of obstructed kidney medulla, increased neuronal NOS (nNOS), and endothelial NOS (eNOS) isoforms expression and COX-2 protein expression in obstructed kidney cortex showed down-regulation of iNOS, nNOS, and COX-2 with persistent levels of eNOS after losartan administration.

Conclusion. These results allowed us to infer an interstitial fibrogenesis prevention independent action of losartan, involving NOS isoforms and COX-2, in unilateral obstructive nephropathy.

Key words: unilateral ureteral obstruction, NOS isoforms, COX-2, TGF-β, losartan, tubulointerstitial fibrosis.

Received for publication September 25, 2003
and in revised form November 20, 2003, and December 18, 2003
Accepted for publication January 28, 2004

The pathologic mechanism underlying chronic obstructive nephropathy is not completely elucidated, although the fibrogenic process clearly plays a critical role in ultimately leading to permanent loss of the normal structural and functional integrity of the kidney [1, 2]. Unlike most forms of chronic renal diseases, often taking months to establish fibrotic lesions, obstructive nephropathy induced by complete, continous ureteral obstruction, is an exceptionally aggressive form of tubulointerstitial fibrosis [3]. Renal fibrogenesis initiates at a very early stage after ureteral obstruction and progresses rapidly [4]. Angiotensin II plays a central role in the initiation and progression of renal disease by autocrine, paracrine, intercrine, and endocrine pathways. Intrarenal concentrations of angiotensin II increase rapidly after the onset of ureteral obstruction in the ligated obstructed kidney. Increased plasma renin activity and renin content, angiotensin-converting enzyme (ACE) and angiotensin II concentration in the experimental kidney are associated with unilateral ureteral obstruction (UUO) [5]. Angiotensin II has been shown to mediate overexpression of transforming growth factor-β (TGF-β) gene, a major cytokine in the regulation of extracellular matrix (ECM) protein synthesis [6]. Significant blunting of this process with ameliorating tubulointestitial fibrosis by an ACE inhibitor and angiotensin II receptor antagonist (AT_1) has been previously reported [7, 8]. In addition, angiotensin II has been shown to up-regulate the expression of a cytokine, tumor necrosis factor-α (TNF-α) [9]. Exposure of kidney epithelial cells from proximal tubule and inner medullary collecting duct (IMCD) to TNF-α increases the level of inducible nitric oxide synthase (iNOS) mRNA [10]. Stimulation of NOS expression by angiotensin II has also been shown in endothelial cells [11]. Evidence also suggests that iNOS may

be expressed under basal conditions in some tissues. Basal expression of iNOS mRNA has been detected in several normal tissues from adult rats [12]. The constitutive NOS isozymes are constantly expressed but are inactive until intracellular Ca^{2+} levels increase sufficiently to maintain calmodulin binding [13]. Notwithstanding neuronal NOS (nNOS) and endothelial NOS (eNOS) are classified as constitutive enzymes, the increased renal vascular resistance, that enhances shear stress and hypoxia, is involved in the constitutive NOS (cNOS) isoform expression in obstruction [14]. Previous studies have shown that endogenous levels of nitric oxide can influence the formation of prostaglandins. Prostaglandins and nitric oxide are important mediators of inflammation. Stimulation of a wide variety of cell types with cytokines and other messengers results in a rapid induction of iNOS and prostaglandins. In cells expressing both inducible prostaglandin endoperoxide synthase (PGHS) and NOS, nitric oxide stimulates prostaglandin production [15]. Regulation of cyclooxygenase-2 (COX-2) gene expression by nitric oxide has been demonstrated in mesangial cells in which nitric oxide donors up-regulated interleukin (IL)-1B–driven COX-2 mRNA and protein expression [16].

A target for intervention in the fibrotic and apoptotic processes in obstruction may be the complex interaction of nitric oxide and TGF-β, induced by angiotensin II, in renal epithelial cells [17]. Recently, prostaglandins have been reported to alter ECM formation by mesangial cells. In addition, a significant reduction of tissue TGF-β by the inhibition of COX-2 has been shown [18].

This study examines the AT_1 angiotensin II receptor inhibition independent from its effects on blood pressure, on NOS isoforms and COX-2 expression, and the significance of this interaction on interstitial fibrosis in UUO.

METHODS

Experiments were performed in female Wistar Kyoto rats with an average body weight of 180 g ($N = 108$). The animals were fed a standard laboratory diet and water ad libitum. Animals were randomly assigned to the group that received a specific inhibitor of the AT_1 angiotensin II receptor [19]. Losartan was administered in the drinking water at 10 mg/kg/day for 15 days, and the other group received plain water. Blood pressure was measured in both groups before and after pharmacology treatment by means of an Pletismografic Grass method (Quincy, MA, USA). After these 2 weeks of losartan administration, UUO was performed in half of rats of the losartan group and in half of the water drinking group. Four groups were formed, on each of the four groups 27 rats were included. Group I included UUO rats without losartan administration, group II were control rats and received no losartan administration; group III were UUO rats given oral losartan administration for 15 days; and group IV were control rats given losartan administration for 15 days.

Animal model of UUO

Urinary tract obstruction of the left kidney of female Wistar Kyoto rats was performed as follows. Animals were first anesthetized with pentobarbital 50 mg/kg body weight intraperitoneally**,** using an aseptic technique, and a midline abdominal incision was performed. The left ureter was completly ligated with 4.0 silk at the upper two thirds of the ureter. The abdominal incision was closed with sutures, the rats were allowed to awaken and were given free access to water and food. The control group underwent a fictitious surgery. Ureteral obstruction was confirmed by observation of dilation of the pelvis and proximal ureter and collapse of the distal ureter at 24 hours. Twenty-four hours later the obstruction was released by removal of the ligature. Clearance studies were done on the day of the obstruction release. Rats ($N =$ 6 on each group) were anesthetized and catheters were placed in the femoral vein and artery and both ureters. In rats from groups I and III, the release of ureteral obstruction was performed by cannulating the obstructed ureter proximal to the ligature placed 24 hours earlier. Rats were placed in plexiglass holders and a period of 1 hour was allowed for recovery from anesthesia. Then a priming dose of inulin (Sigma Chemical Co., St. Louis, MO, USA) dissolved in normal saline (0.6 to 1 mL) was infused over 3 minutes. It was followed by a sustaining infusion of inulin in normal saline given at a rate of 40 μL/min designed to result in serum concentration of inulin of 75 to 100 mg/dL.Two hours after the infusion was started, three consecutive collections of urine of 30 minutes each was obtained. Urine volume was determined by weighing the urine collected in previously weighed tubes. Blood was drawn at the beginning, midpoint, and end of each clearance period, collected in heparinized microhematocrit capillary tubes. Mean arterial pressure (MAP) was determined through the left femoral artery catheter connected to a manometer.Two successive readings were obtained. After completing the clearance studies, the animals were anesthetized and perfusion through the aorta with cold phosphate-buffered saline (PBS) was performed. Kidneys were rapidly removed and sliced on a cold glass plate.

For histologic studies, kidney sections were fixed in 10% phosphate-buffered formalin (pH = 7.1) for 24 to 48 hours before embedded in paraffin and serially sectioned (5 μm) on a microtome (Leica, Nussloch, Germany). Paraffin sections were subjected to staining with hematoxylin-eosin and Masson trichromic.

Kidney sections were treated sequentially with Weigert's iron hematoxylin solution × 10 minutes, Biebrich scarlet–acid fuchsin × 2 minutes, phosphotungstic acid/phosphomolybdic acid × 10 minutes, and aniline blue × 5 minutes for Masson trichromic staining. Tissue was destained in 1% acetic acid × 2 minutes, dehydrated through graded ethanol to xylene, and mounted for examination by light microscopy [20].

Morphometric evaluation of interstitial fibrosis

For all morphologic evaluations the observer was naive to the origin of the histologic sections. A standard point counting method [21, 22] was used to quantitate the volume of the renal interstitium. The relative volume (Vv) of the renal cortical interstitium was determined in sections by using the Masson trichrome method to stain collagen fibers. Blue-stained interstitial fibrotic areas were assessed by using an image analyzer (Image Pro-Plus 4.0; Media Cybernetics, Silver Spring, MD, USA). Ten consecutive fields were randomly selected in renal cortex and medulla and were evaluated at 400 × on a 10 × 10 grid-imprinted reticule. All points not counted within tubular cells, lumen, glomeruli, or vascular space were considered interstitial. This fraction represented the relative interstitial volume. The number of grid points containing blue collagen staining in the interstitium was divided by the total number of points in the fields (1000) to obtain the percentage fractional area of interstitial collagen deposition.

Results were expressed as percentage of the measured area, which represented the interstitial space and was determined as the relative volume (Vv) of the interstitium.

Tubular diameter in renal cortex and medulla

Tubule atrophy has been previously determined by measuring tubule diameter, which would be an index of all apoptotic cell loss - atrophic tubules were identified by their thickness [22].

To evaluate if atrophy affected 24-hour kidney obstruction tubules, measurement of tubule diameter on kidney sections stained with Masson trichromic was performed.

The diameter of the tubules per field of a 40 × objective was determined in the same 10 fields of cortex and medulla per kidney section in which the relative volume (Vv) of the interstitium was measured. Tubular diameter was assessed by using an image analyzer (Image Pro-Plus 4.0).

Preparation of kidneys for NOS activity and RNA extraction

The kidneys were perfused from the abdominal aorta with 25 mL of cold PBS solution to rinse all the blood. For the determination of NOS activity, a protocol for homogenates was performed.

Slices from kidneys ($N = 10$ in each group) were done and renal cortex and medulla were removed under a stereomicroscope. After weighing both the cortex and the medulla, they were immediately frozen on dry ice. Later, tissues were homogenized by using a glass microhomogenator (Lighting Model Mixer-Volts 100) (Mixing Equipment Co., Inc., Rochester, NY, USA.) in a cool solution (10 mg tissue/100 μL solution) containing Hepes-Tris10 mmol/L, sacarose 0.32 mol/L, dithiothreitol (DTT) 1 mmol/L, soybean trypsin inhibitor 1 mg/100 mL, and trasylol 2.5 μg/mL to pH = 7.40. Cortex and medulla homogenates of each kidney were used for the measurement of inducible and constitutive isoforms of NOS enzyme.

Measurement of NOS activity

NOS activity was quantified by measuring the conversion of L-[^{3}H] arginine to L-[^{3}H] citrulline in the presence of saturating concentrations of the enzyme's cofactors as it was described before [23] with brief modifications.

Homogenates from renal cortex and medulla were centrifugated at 3000 rpm at 4°C for 10 minutes. A 40 μL aliquot of each supernantant fraction was incubated with 3 mmol/L $CaCl_2$, 1 mmol/L β-nicotinamide adenine dinucleotide reduced form (NADPH), 25 μmol/L flavin adenine dinucleotide (FAD), 1.25 μg/mL calmodulin, 10 μmol/L tetrahydrobiopterin, and [^{3}H] arginine (approximately 300,000 cpm, 6.8 Ci/mL) in 20 mmol/L Hepes buffer, pH = 7.40, at 37°C for 30 minutes. Calcium/calmodulin-independent NOS activity was measured by using the same buffer and cofactors, without calcium and calmodulin, after the addition of 0.5 mmol/L ethylenediaminetetraacetic acid (EDTA). Parallel reactions were analyzed in the presence of N^G-nitro-L-arginine methyl ester (L-NAME) 20 mmol/L, an inhibitor of inducible and constitutive isoforms NOS in renal cortex and medulla of control kidneys. The reaction was stopped by the addition of L-NAME 20 mmol/L Hepes buffer (100 μL) at 4°C. The total volume (210 μL) was applied to a Dowex 50W-X8, 100 to 200 mesh column (volume 0.6 mL) that had been pre-equilibrated with 20 mmol/L Hepes (pH = 7.40) and saturated with 20 mmol/L of cold citrulline. [^{3}H] citrulline was eluted with 200 μL of deionized water and radioactivity was quantified by scintillation counting (Wallac, LK Beta Rack, Finland). Blanks included 50 μL of homogenate buffer plus 60 μL of reaction buffer without or with calcium/calmodulin to measure iNOS and cNOS respectively. The results are expressed as fmol [^{3}H] citrulline/min incubation/μg protein.

Protein concentrations were measured according to Bradford [24] by using Bio-Rad reagent (Bio-Rad Laboratories, Hercules, CA, USA). Bovine serum albumin (BSA) was used as standard (1 mg/mL).

RNA isolation, reverse transcription-polymerase chain reaction (RT-PCR), and semiquantification for NOS isoforms

For RNA extraction, kidneys ($N = 6$ in each group) were rapidly removed and cortex and medulla dissected immediately. Total RNA was prepared by using Trizol reagent (from Gibco, BRL, Life Technologies, Gaithersburg, MD, USA). The total RNA was dissolved in RNAse-free water (Promega, Madison, WI, USA) and quantitated by ultraviolet spectrophotometry at 260 nm and 280 nm. RNA with an optical density (OD) 260/OD 280 ratio between 1.7 to 1.9 was used for cDNA synthesis.

Three to five micrograms of RNA have been denaturated in the presence of 0.5 mg/50mL oligo $(dT)_{15}$ primer and 40 U recombinant ribonuclease inhibitor (RNasin) (Promega). RT was performed in the presence of mixture by using 200 U Reverse Transcriptase Moloney-murine leukemia virus (M-MLV) RT in reaction buffer (Promega), 0.5 mmol/L deoxynucleoside triphosphate (dNTP) each, and incubating 60 minutes at 37°C. The cDNA (15 μL) was amplified by PCR. Each sample was measured for iNOS, nNOS, eNOS, and β-actin cDNA in separate tubes using 50 pmol specific primers. The upstream and downstream primers for iNOS were 5′-GCAT GGACCAGTATAAGGCAAGCA-3′ and 5′-GCTTCT GGTCGATGTCATGAGCAA-3′, respectively. These yield a single band corresponding to a 222 bp fragment. Analysis of the sequence revealed that it was identical to position 1693–1915 in mouse macrophage iNOS cDNA [25].The upstream and downstream primers for nNOS were 5′-GAACCCCCAAGACCATCC-3′ and 3′-GGC TTTGCTCCCACAGTT-5′, respectively, which yield a single band corresponding to a 308 bp cDNA fragment [26]. The upstream and downstream primers for eNOS (325 bp) were 5′-CTACAGAGCAGCAAATCC ACCCG-3′ and 5′-AGCAGTCGAAGGAGGCGAGG ACTAG-3′, respectively. These primers were designed by Dr. María Rüttler by using the PC/Gene (the nucleic acid and protein sequence analysis software system from the University of Geneva/Switzerland IntelliGenetics, release 6.85/1995, serial number IGI 3481).

The upstream and downstream primers for β-actin was 5′-TGGAGAAGAGCTATGAGCTGCCTG-3′ and 5′-GTGCCACCAGACCAGCACTGTGTTG-3′, respectively, which yield a single band corresponding to a 201 bp cDNA fragment. Amplification of a fragment of β-actin was done so as to evaluate nonspecific effects of the experimental conditions and to semiquantitate NOS isoforms expression PCR was performed by incubating 15 μL of sample cDNA with 50 mmol/L KCl Tris-ClH, 0.1% gelatin, 1.5 mmol/L $MgCl_2$, 2 U Taq polymerase, 100 pmol of β-actin or iNOS primers in 50 μL final volume PCR reaction was carried out for 30 cycles for iNOS, nNOS, and β-actin (denaturation 1 minute at 94°C, annealing 1 minute at 55°C and 2 minutes extension step at 72°C, followed by a final extension step of 3 minutes at 72°C).

RT-PCR for TGF-β

The mixture of total RNA 3 to 5 μg/10 μL RNAase-free water, and 0.5 mg/50mL oligo (dT) was incubated at 65°C for 10 minutes to denature the secondary structure and chilled in ice immediately. The resulting mixture was incubated at 42°C for 1 hour adding 200 U of Reverse Transcriptase M-MLV RT in reaction buffer (Promega), heated at 94°C for 5 minutes and chilled on ice. The cDNA (15 μL) was amplified by PCR. Amplification was done in a total volume of 50 μL containing PCR buffer (50 mmol/L KCl, 10 mmol/L Tris-HCl, 2 mmol/L $MgCl_2$, 200 μmol/L dNTP, 1.25 U Taq DNA polymerase, 100 pmol of β-actin or 50 pmol of oligonucleotide primers for TGF-β. The TGF-β primers were designed from the sequence of the rat gene sense 5′-GGACTAC TACGCCAAAGAAG-3′ (bp 715–734) and antisense 5-TCAAAAGACAGCCACTCAGG-3′ (bp 989–1008). The anticipated PCR product was 294 bp in length [27].

To quantitate PCR products and to confirm the integrity of RNA, we coamplified a housekeeping gene, β-actin in companion tubes. PCR was performed with a DNA Thermal Cycler (Minicycler MJ Research, Beverly, MA, USA) with the following program: 95°C for 1 minute (denaturing), 54°C for 1 minute (annealing), and the extension phase at 72°C for 1 minute. The reaction was followed by a final elongation step at 72°C for 7 minutes. Controls with no added RT were run in parallel to rule out genomic contamination. Amplification was carried out at 30 cycles for TGF-β and for β-actin.

Relative quantitation of mRNA

To 15 μL of the final product, PCR was electrophoresed by using 1.5% agarose gel in Tris-boric acid-EDTA (TBE) buffer. Gels were stained with 1 mg/mL ethidium bromide, visualized with an ultraviolet transluminator UV (Cole Parmer Instruments, Inc., Chicago, IL, USA) and photographed.The photograph was digitized by using a scanner (Lacie Silver Scanner for Macintosh) and the Desk Scan software (Adobe PhotoShop) on a desktop computer. The image was inverted before performing densitometric analysis by using National Institutes of Health Image 1.6 software (Wayne et al, Division of computer Research and Technology, NIH, Bethesda, MD, USA).

The NOS isoforms signals were standardized against β-actin signal for each sample, and results were expressed as each NOS isoform/β-actin ratio, respectively. The PCR products of TGF-β and β-actin were also electrophoresed in the same gel and ratio for TGF-β/β-actin for each sample was determined.

Autoradiography for angiotensin II receptors

A total of 20 rats were used for radioligand binding studies. Immediately after the animals were killed, kidneys from control and unilaterally obstructed animals before and after losartan treatment were removed, weighed, and frozen in isopentane. The kidneys were stored at –70°C. Tissues were used for autoradiography and within 2 weeks the animals were sacrificed. The kidneys placed on dry ice and cut into 16 μm thick slices with the aid of a cryostat. The sections were collected on gelatin-coated microscope slides and kept on a dessicator overnight at 4°C. The sections were incubated in vitro with 0.2 nmol/L [^{125}I] Sar-1, Ile-8 angiotensin II (Amersham Pharmacia Biotech Code IM248, Buckinghamshire, UK), activity 2000 Ci/mmol, as described in previous work [28]. Briefly, sections were preincubated during 15 minutes at room temperature in 10 mmol/L sodium phosphate buffer, pH = 7.4, containing 120 mmol/L NaCl, 5 mmol/L disodium EDTA, 0.005% bacitracin (Sigma Chemical, Co.) and 0.2% BSA fraction V (Sigma Chemical Co.) followed by an incubation for 120 minutes in fresh buffer containing the ligand. After the incubation period, the slides were rinsed four consecutive times, 1 minute each, in fresh ice-cold 50 mmol/L Tris-HCl buffer, pH = 7.6, followed by a 30-second rinse in ice-cold water and allowed to dry overnight on a dessicator under vacuum. For angiotensin II subtype identification, consecutive sections were incubated with the ligand in the presence of 1×10^{-5} mol/L of AT_1 losartan (code MRL-459/4 donated by Roemmers Laboratory), to define AT_2 receptors, or 1×10^{-5} mol/L PD123319 ditrifluoroacetate (Sigma Chemical Co.), to define AT_1 subtype. Nonspecific binding was defined by incubating in the presence of 5×10^{-6} mol/L angiotensin II acetate (Sigma Chemical Co.). The dried labeled sections were overlay to 3H-Hyperfilm (Amersham, Arlington Heights, IL, USA) in x-ray cassettes. Together with a set of ^{14}C standard (Amersham Pharmacia Biotech), films were developed with Kodak GBX developer and fixer after 4 to 7 days' exposure. Densitometric analysis was performed by digitalization of the images and curve fitting made with the aid of the NIH Image program, 1.6/ppc. Values are expressed in fmol/mg protein by using a correction factor that includes the equivalence of milligram of plastic polymer of the standards with the protein content in the tissue.

Immunoblotting analysis for COX-2

Renal cortex and medulla were homogenized in 50 mmol/L Tris-HCl (pH = 7.8) lysis buffer containing 0.01% Triton X-100 and protease inhibitor cocktail. After that, the homogenates were centrifuged at 4°C, 11,000 rpm, for 30 minutes. Protein concentrations of the resulting supernatants were determined by Lowry method by using BSA as standard [29]. Forty micrograms of proteins were mixed with 10 μL of sample buffer [125 mmol/L Tris-HCl, pH = 6.8, 4% sodium dodecyl sulfate (SDS), 3.5 mmol/L DTT, 0.02% bromophenol blue and 20% glycerol], boiled for 2 to 3 minutes, and loaded into an 8% SDS-polyacrylamide gel elctrophoresis (PAGE) gel. Protein molecular mass markers were always loaded on each gel. The protein bands were transferred into a polyvinylidine difluoride (PVDF) membranes (Polyscreen NEF 1000), which were purchased from NEN Life Science Products using a blot transfer system (Bio-Rad Laboratories). After being blocked with 5% BSA and Tris-buffered saline (TBS) solution (20 mmol/L Tris and 500 mmol/L NaCl, pH = 7.5) overnight, at 4°C with gentle agitation, membranes were incubated with a primary rabbit anti-COX-2 polyclonal antibody solution (Santa Cruz Biotechnology, Santa Cruz, CA, USA) (1:1000 dilution) for 1 hour at room temperature. After washing three times with TTBS (0.1% Tween 20, 100 mmol/L Tris-HCl, pH = 7.5, and 150 mmol/L NaCl), membranes were incubated with an antirabbit IgG secondary antibody linked to biotin for 1 hour at room temperature [30]. Membranes were washed twice and the color was developed by using a Vectastain ABC 8211detection system.

After exposure to x-ray film, the photograph was digitized using a scanner (Lacie Silver Scanner for Macintosh) and the Desk Scan software (Adobe PhotoShop) on a desktop computer as previously described.

Statistical analysis

The results were assessed by one-way analysis of variance (ANOVA) for comparisons among groups. Significance of differences was estimated by Bonferroni test. A $P < 0.05$ was considered to be significant. Student t test was performed to compare the means when the experimental design consisted of two samples. Statistical significance was assessed by Student impaired t test.

A $P < 0.05$ was considered to be significant. Results are given as means ± SEM. Statistical tests were performed by using GraphPad In-Stat, version 3.00, for Windows 95 (GraphPad Software, Inc., San Diego, CA, USA).

RESULTS

Oral administration of losartan during 15 days had no effect on blood pressure in obstructed and control rats (111.9 ± 2.2 mm Hg vs. 110.4 ± 2.2 mm Hg, and 110.4 ± 2.2 mm Hg vs. 112.7 ± 3.2 mm Hg, respectively). Body and kidney weights were similar among groups. Data are included in Table 1.

To assess the effect of losartan on renal function, we performed renal clearance studies in each of the kidneys of six rats of the four groups. Table 1 shows that glomerular filtration rate (GFR) was intensively decreased in the post-obstructed kidneys of vehicle-treated animals compared with sham-operated rats ($P < 0.001$). Recovery of

Table 1. Blood pressure, body weight, kidney weight, and glomerular filtration rate (GFR) in unilateral ureteral obstruction (effect of AT_1 angiotensin II receptor inhibition)

Parameters	Group I		Group II	Group III		Group IV
	Obstructed kidney	Contralateral kidney	Control kidney	Obstructed kidney	Contralateral kidney	Control kidney
Weight *g*	195.80 ± 3.20		194.60 ± 4.30	195.40 ± 4.00		196.80 ± 5.00
Kidney weight *mg*	590 ± 31.20	547 ± 7.30	520.30 ± 10.50	580.80 ± 17.20	540.40 ± 30.30	525.50 ± 10.30
Blood pressure *mmHg*	94.80 ± 2.60		97.70 ± 3.40	96 ± 0.60		98.60 ± 2.88
GFR *mL/min*	0.25 ± 0.05[a]	1.22 ± 0.10	0.90 ± 0.08	0.592 ± 0.06	1.09 ± 0.06	0.88 ± 0.06

Groups I and II, Unilateral ureteral obstructed rats and control rats without Losartan treatment; groups, III and IV, Unilateral ureteral obstructed rats and control rats pretreated with Losartan (oral dose of 10 mg/kg) for 15 days.

Values are means ± SEM.

[a] $P < 0.01$ GFR in postobstructed kidneys without losartan ($N = 6$) vs. GFR in control kidneys ($N = 6$).

Where in table $P < 0.05$ GFR in postobstructed kidneys without losartan vs. GFR in postobstructed kidneys with losartan ($N = 6$).

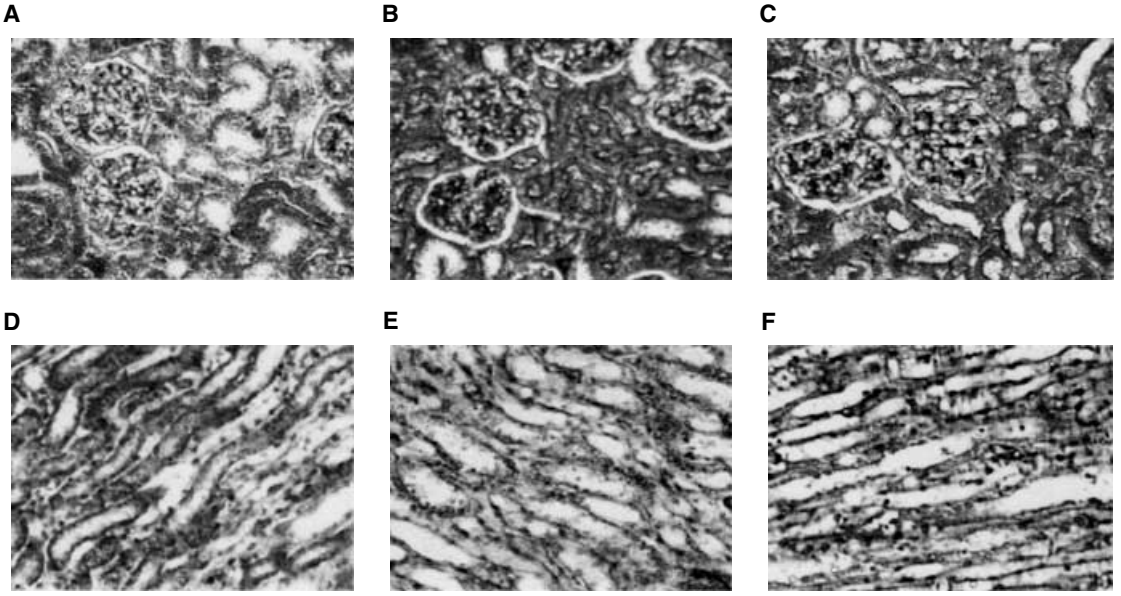

Fig. 1. Trichromic-Masson stained sections of rat kidney cortex and medulla. (*A*) Sham-operated kidney cortex. (*B*) Ureter-obstructed untreated kidney cortex. (*C*) Ureter-obstructed, losartan-treated kidney cortex. (*D*) Sham-operated kidney medulla. (*E*) Ureter-obstructed untreated kidney medulla. (*F*) Ureter-obstructed, losartan-treated kidney medulla (magnification 400×).

GFR was observed in losartan-treated group with obstruction ($P < 0.05$). The GFR of the contralateral kidneys tended to be increased in the losartan-treated group similar to that of the vehicle group, compared with the sham one. No significant differences on MAP were observed among groups (Table 1).

Morphology of the renal cortex and medulla

We analyzed the degree of tubulointerstitial fibrosis after 24 hours of UUO in cortical and medullary sections of rat kidneys subjected to the treatment with vehicle or losartan, as described in the **Methods** section. Masson's trichrome-stained sections were used to analyze the accumulation of collagen in the interstitium. With this stain, collagen was colored blue. Collagen was detected in Bowman's capsule, in the basement membrane surrounding tubules in mesangial matrix, and in capillaries of control kidneys, as it has been previously shown [21]. In comparison, kidneys subjected to UUO for 24 hours had higher accumulation of collagen in the expanded interstitium along with cellular interstitial infiltrates in the cortex and medulla. Contralateral, nonligated kidneys in all of the experimental groups were indistinguishable from normal kidneys. Kidneys from rats treated with losartan for 15 days before the obstruction surgery had less interstitial collagen deposition compared to kidneys subjected to UUO (Fig. 1).

Morphometric analysis of tubulointerstitial volume

The volume of the interstitial fibrotic area relative to the cortical tubulointerstitial area was expressed as the volume fraction (Vv). The interstitial volume of the obstructed cortex kidney revealed a twofold expansion of the interstitial space compared to control, from 13.7 ± 1.5

to 28 ± 2.6 ($P < 0.01$) of the cortical volume. In the group of rats given losartan before unilateral obstruction, the expansion of the interstitial space was significantly decreased 28 ± 2.6 vs. 20.7 ± 1.2 ($P < 0.01$). Increased interstitial volume fraction (Vv) was also demonstrated in obstructed medulla compared to control medulla 32 ± 3.8 vs. 5.5 ± 1.8 ($P < 0.01$). After losartan administration, lower volume fraction (Vv) was shown in obstructed kidney medulla 32 ± 3.8 vs. 19 ± 2.7 ($P < 0.01$). No significant difference was observed in Vv of the contralateral cortex and medulla kidneys from groups I and III related to control.

Tubular diameter in renal cortex and medulla

Determination of tubule diameter was carried on from the same sections in which interstitial volume was measured. The average tubule diameter in sections of obstructed cortex kidneys ($N = 6$) was similar to that of the kidneys of the sham group 21.4 ± 4 μm vs. 21.2 ± 2 μm. No tubular atrophy was demonstrated in obstructed kidneys. Slight increase in tubular diameter was found in obstructed medullas related to control 22.1 ± 4 μm vs. 17.1 ± 2 μm ($P < 0.05$). Losartan induced no changes on tubular diameter on obstructed cortex 21.4 ± 4 μm vs. 22.5 ± 4 μm and medulla 22.1 ± 4 μm vs. 20.5 ± 1.2 μm, respectively.

NOS activity on renal medulla tissue in obstruction: Effect of losartan

NOS activity was measured by the conversion of L-[^{3}H] arginine to L-[^{3}H] citrulline. When homogenates from renal medulla tissue of obstructed kidneys without losartan (group I, $N = 10$) were incubated in the presence of saturating concentrations of the enzyme cofactors, a significant increase in the activity of calcium/calmodulin-independent NOS (iNOS) when compared to contralateral kidney (0.675 ± 0.04 fmol [^{3}H] citrulline/min/μg protein vs. 0.237 ± 0.04 fmol [^{3}H] citrulline/min/μg protein) ($P < 0.001$) and control kidney (group II, $N = 10$) (0.675 ± 0.04 fmol [^{3}H] citrulline/min/μg protein vs. 0.313 ± 0.01 fmol [^{3}H] citrulline/min/μg protein) ($P < 0.001$) was demonstrated. Although an increase on calcium/calmodulin-dependent NOS (cNOS) activity (fmol [^{3}H] citrulline/min/μg protein) was observed in obstructed medulla related to medulla of control kidneys without losartan (group II) (0.381 ± 0.03 vs. 0.198 ± 0.03) ($P < 0.01$), higher iNOS activity in comparison to cNOS activity was shown on the obstructed medulla 0.675 ± 0.04 vs. 0.381 ± 0.03 ($P < 0.001$) (Fig. 2).

Slight increase was observed on calcium/calmodulin-dependent NOS activity in the medulla of the obstructed rat kidney without losartan (group I) compared to medulla of contralateral kidneys (0.381 ± 0.03 fmol [^{3}H] citrulline/min/μg protein vs. 0.240 ± 0.02 fmol [^{3}H] citrulline/min/μg protein) ($P < 0.05$) (Fig. 2).

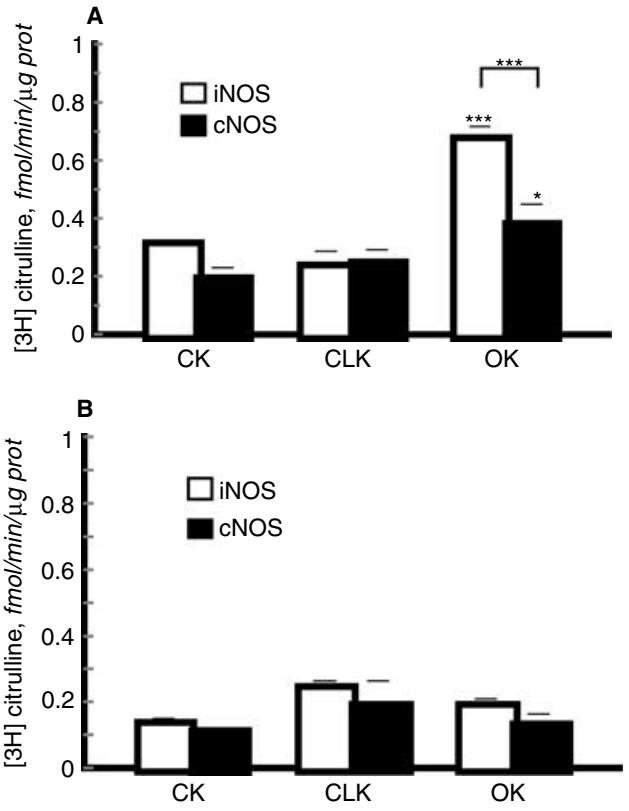

Fig. 2. Effect of oral losartan 10 mg/kg on nitric oxide synthase (NOS) activity in rat renal medulla. (*A*) Calcium/calmodulin NOS activity in obstructed kidneys (OKs) ($N = 10$) in animals of groups I and II (without losartan treatment) related to control kidneys (CKs) ($N = 10$; $^{***}P < 0.001$) and contralateral kidneys (CLKs) ($N = 10$; $^{***}P < 0.001$) for independent inducible NOS activity (iNOS), and for dependent constituitive NOS activity (cNOS) in obstructed kidneys ($N = 10$) related to control kidneys ($N = 10$; $^{***}P < 0.001$) and contralateral kidneys ($N = 10$ $^{*}P < 0.05$). Higher iNOS activity related to cNOS activity ($^{***}P < 0.001$) on the obstructed medulla without losartan [one-way analysis of variance (ANOVA) test]. Values are means ± SEM. (*B*) Calcium/calmodulin NOS activity (iNOS and cNOS) in obstructed kidneyss, contralateral kidneys, and control kidneys ($N = 10$) after losartan administration. Decrease on calcium/calmodulin-independent (iNOS) and dependent NOS (cNOS) activity in obstructed kidneys ($N = 10$) after losartan administration related to the activity on obstructed kidneys without losartan ($N = 10$; $^{***}P < 0.001$), respectively. Group III vs. group I (Student impaired *t* test). Values are means ± SEM.

Homogenates from renal medulla tissue of obstructed kidneys with Losartan (group III, $N = 10$) induced a decrease of iNOS activity when compared to medulla of obstructed kidneys without losartan (0.190 ± 0.02 fmol [^{3}H] citrulline/min/μg protein vs. 0.675 ± 0.04 fmol [^{3}H] citrulline/min/μg protein) ($P < 0.01$). Decrease on calcium/calmodulin-dependent NOS activity was also observed in the renal medulla of obstructed kidney with losartan (group III) related to the renal medulla of obstructed kidney without losartan (group I) (0.133 ± 0.03 fmol [^{3}H] citrulline/min/μg protein vs. 0.381 ± 0.03 fmol

[^{3}H] citrulline/min/μg protein) ($P < 0.01$). No differences in homogenates of the renal medulla of contralateral kidneys with losartan (group III) compared to the one of the medulla of contralateral kidneys without losartan (group I) were observed in calcium/calmodulin-independent activity (0.243 ± 0.02 fmol [^{3}H] citrulline/min/μg protein vs. 0.237 ± 0.04 fmol [^{3}H] citrulline/min/μg protein and calcium/calmodulin-dependent NOS activity (0.190 ± 0.01 fmol [^{3}H] citrulline/min/μg protein vs. 0.240 ± 0.04 fmol [^{3}H] citrulline/min/μg protein). Measurement of calcium/calmodulin-independent NOS activity (fmol [^{3}H] citrulline/min/μg protein) on homogenates of the renal medulla of control kidneys with losartan (group IV, $N = 10$) showed a decreased activity compared to control kidney medullas without losartan, group II (0.137 ± 0.01 vs. 0.313 ± 0.01 ($P < 0.01$), no differences were observed on contralateral medulla pretreated with losartan related to nontreated contralateral kidney 0.111 ± 0.01 fmol [^{3}H] citrulline/min/μg protein vs. 0.198 ± 0.03 fmol [^{3}H] citrulline/min/μg protein (Fig. 2).

NOS activity on renal cortex tissue in obstruction: Effect of losartan

No differences were observed on calcium/calmodulin-independent NOS activity among renal cortex of obstructed, contralateral, and control kidneys without losartan (groups I and II) 0.221 ± 0.02 vs. 0.235 ± 0.02 vs. 0.224 ± 0.01 (fmol [^{3}H] citrulline/min/μg protein).

Homogenates of renal cortex of obstructed kidneys without losartan (group I) showed a slight increase on calcium/calmodulin-dependent NOS (cNOS) activity (fmol [^{3}H] citrulline/min/μg protein), when compared with renal cortex of control kidneys without losartan, group II (0.396 ± 0.08 vs. 0.191 ± 0.03) ($P < 0.01$) and contralateral kidneys without losartan (0.396 ± 0.08 vs. 0.194 ± 0.03) ($P < 0.01$). Higher cNOS activity compared to iNOS activity in obstructed kidney was shown ($P < 0.05$) (Fig. 3).

After losartan administration, no differences were observed on calcium/calmodulin-independent NOS activity related to obstructed kidney without losartan: iNOS 0.225 ± 0.03 fmol [^{3}H] citrulline/min/μg protein vs. 0.221 ± 0.02 fmol [^{3}H] citrulline/min/μg protein. On the contrary, decreased activity was observed on calcium/calmodulin-dependent activity in obstructed cortex after losartan compared to nontreated obstructed cortex 0.160 ± 0.04 fmol [^{3}H] citrulline/min/μg protein vs. 0.396 ± 0.08 fmol [^{3}H] citrulline/min/μg protein ($P < 0.001$). No differences were observed on calcium/calmodulin-independent and dependent NOS activity in contralateral and control kidneys after the administration of losartan for 15 days, before unilateral obstruction for 24 hours compared to basal conditions contralateral cortex, iNOS 0.207 ± 0.02 fmol [^{3}H] citrulline/min/μg protein vs. 0.235 ± 0.02 fmol [^{3}H] citrulline/min/μg protein; cNOS 0.184 ± 0.02 fmol [^{3}H] citrulline/min/μg protein vs. 0.194 ± 0.03 fmol [^{3}H] citrulline/min/μg protein groups I and III; control cortex, iNOS 0.145 ± 0.02 fmol [^{3}H] citrulline/min/μg protein vs. 0.224 ± 0.01 fmol [^{3}H] citrulline/min/μg protein; cNOS 0.153 ± 0.003 fmol [^{3}H] citrulline/min/μg protein vs. 0.191 ± 0.03 fmol [^{3}H] citrulline/min/μg protein, groups II and IV (Fig. 3).

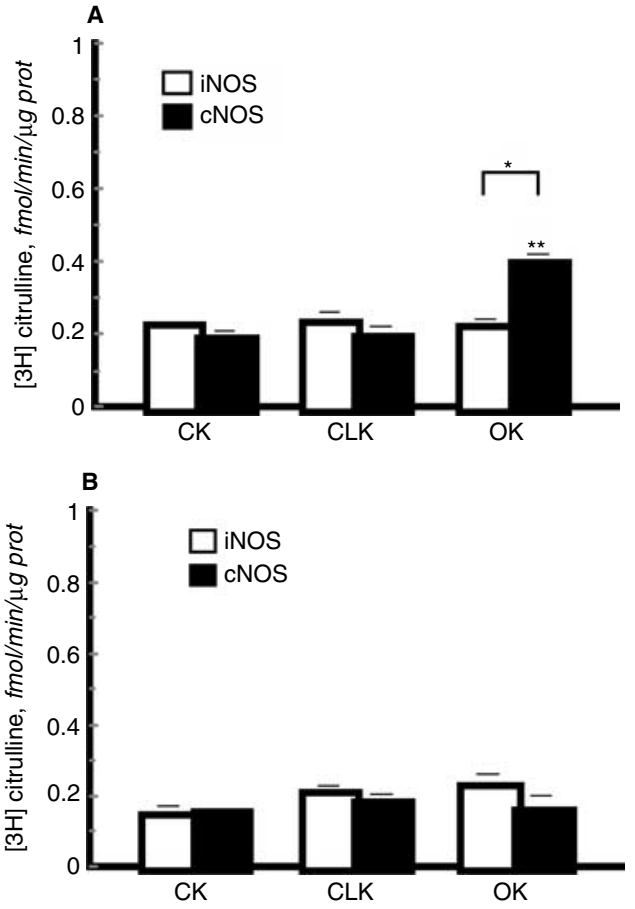

Fig. 3. Effect of oral losartan 10 mg/kg on nitric oxide synthase (NOS) activity in rat renal cortex. (*A*) Calcium/calmodulin-independent inducible NOS activity (iNOS) in obstructed kidneys (OKs) ($N = 10$), control kidneys (CKs) ($N = 10$), and contralateral kidneys (CLKs) ($N = 10$) without losartan administration. Increased calcium/calmodulin-dependent constituitive NOS activity (cNOS) in obstructed kidneys ($N = 10$) related to control kidneys ($N = 10$; $^{**}P < 0.01$) and contralateral kidneys ($N = 10$; $^{**}P < 0.01$). Groups I and II [one-way analysis of variance (ANOVA) test]. (*B*) Decrease on calcium/calmodulin-dependent NOS activity in obstructed kidneys ($N = 10$) after losartan administration related to the activity in obstructed kidneys nonlosartan treated ($N = 10$; $^{***}P < 0.001$). Group III vs. group I (Student impaired *t* test). Values are means ± SEM.

NOS mRNA isoforms expression on renal medulla in obstruction

Under identical conditions, an amount of 3 to 5 μg of total RNA from each renal medulla of obstructed,

contralateral and control kidneys was reverse transcribed. The integrated optical intensity of the RT-PCR product of iNOS, nNOS, and eNOS isoforms fluorescence in the ethidium bromide stain was analyzed. The intensity of the amplified housekeeping gene, β-actin was almost uniform in all tissues, confirming that the efficiency of RT did not vary significantly between samples. The amplified fragment of iNOS (222 bp) was clearly visible in obstructed medulla iNOS expression. Slight detection was demonstrated in contralateral and control medulla. Densitometric analysis of the iNOS mRNA corrected for β-actin expression (relative densitometric units) showed a significant increase on obstructed medulla compared to contralateral kidney 0.852 ± 0.05 vs. 0.614 ± 0.04 ($P < 0.05$) and control kidney 0.852 ± 0.05 vs. 0.538 ± 0.06 ($P < 0.01$). Decrease on iNOS mRNA expression was demonstrated in obstructed medulla kidneys pretreated with the inhibitor of AT_1 receptor of angiotensin II (group III), compared to iNOS mRNA expression in obstructed kidneys without losartan (group I) with a significant lower densitometric ratio iNOS mRNA to β-actin (relative densitometric units) 0.852 ± 0.01 vs. 0.646 ± 0.04 ($P < 0.05$) (Fig. 4).

On the contrary, no differences were observed on the analysis of the nNOS mRNA corrected for β-actin expression on medulla among groups, with a densitometric ratio (relative densitometric units) of nNOS in obstructed kidney 0.714 ± 0.02, contralateral kidney 0.680 ± 0.03, and control kidney 0.672 ± 0.03, respectively (groups I and II).

In obstructed kidney medullas, after losartan, decreased nNOS expression was shown 0.714 ± 0.02 vs. 0.530 ± 0.01 ($P < 0.01$).

There were no changes on iNOS and nNOS signal standardized against β-actin signal (relative densitometric units) for each sample in contralateral medulla after losartan administration, iNOS 0.614 ± 0.08 vs. 0.600 ± 0.01, and nNOS 0.630 ± 0.03 vs. 0.680 ± 0.03. Similar results were obtained in the expression of iNOS in control medulla after losartan 0.538 ± 0.10 vs. 0.521 ± 0.009, decreased nNOS expression was shown on control medulla after AT_1 receptor inhibitor 0.672 ± 0.034 vs. 0.510 ± 0.08 ($P < 0.05$) (groups II and IV).

Densitometric analysis of the eNOS mRNA corrected for β-actin expression (relative densitometric units) showed a significant increase on obstructed medulla compared to control kidney 1.10 ± 0.07 vs. 0.730 ± 0.02 ($P < 0.01$). No difference expression of eNOS was observed on contralateral medulla compared to obstructed medulla 1.27 ± 0.03 vs. 1.10 ± 0.02. After losartan administration no differences were observed on eNOS expression in medulla of obstructed kidney 1.10 ± 0.07 vs. 1.24 ± 0.0, contralateral medulla 0.730 ± 0.02 vs. 0.750 ± 0.02, and control medulla 1.27 ± 0.03 vs. 1.28 ± 0.04 (Fig. 6A).

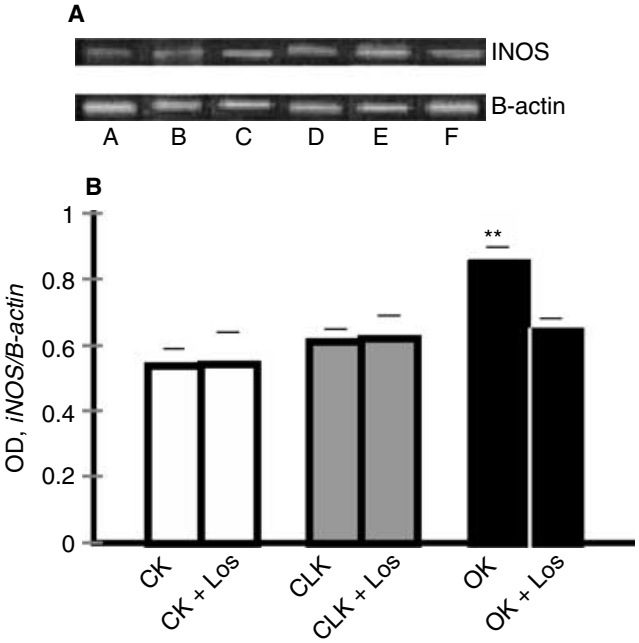

Fig. 4. Expression of inducible nitric oxide synthase (iNOS) and β-actin mRNA in kidney medulla after unilateral ureteral obstruction (UUO). (A) Representative gel of iNOS mRNA in medulla obtained from control (lane A),contralateral (lane C), and obstructed kidney (lane E) 24 hours following UUO. After AT_1 angiotensin II receptor blockade by inhibitor losartan products of reverse transcription-polymerase chain reaction (RT-PCR) for iNOS are shown in lane B (control medulla), lane D (contralateral medulla), and lane F (obstructed medulla). Housekeeping gene β-actin expression is included in below the iNOS expression. These results are typical of six independent observations. (*B*) Semiquantitative PCR analysis of iNOS isoform in renal medulla of UUO, contralateral and control kidneys. Effect of losartan increased iNOS/β-actin mRNA ratio in obstructed kidneys (OKs) ($N = 6$) related to control kidneys (CKs) ($N = 6$; $^{**}P < 0.01$) and to contralateral kidneys (CLKs) ($^{*}P < 0.05$). Increased iNOS/β-actin mRNA ratio in obstructed kidneys ($N = 6$) related to obstructed kidneys with losartan (Los) treatment ($N = 6$; $^{*}P < 0.05$). Values are means ± SEM.

NOS mRNA isoforms expression on renal cortex in obstruction

No differences on the densitometric analysis of iNOS mRNA corrected for β-actin expression (relative densitometric units) in obstructed cortex related to contralateral and control cortex were observed, 0.626 ± 0.06 vs. 0.695 ± 0.03 vs. 0.597 ± 0.04 (groups I and II). The pretreatment with an inhibitor of AT_1 angiotensin II receptor showed no differences on the levels of iNOS signal in obstructed kidneys, 0.658 ± 0.05 vs. 0.626 ± 0.06. No differences on iNOS mRNA corrected for β-actin expression (relative densitometric units) were shown after Losartan treatment on control kidneys, 0.597 ± 0.047 vs. 0.532 ± 0.033 and contralateral kidneys, 0.695 ± 0.038 vs. 0.710 ± 0.016 (groups III and IV).

Cortical nNOS expression was increased in the obstructed kidney compared with control and with contralateral kidney cortex 0.847 ± 0.03 vs. 0.720 ± 0.02 ($P < 0.05$) and 0.847 ± 0.03 vs. 0.680 ± 0.02 ($P < 0.01$) (groups I

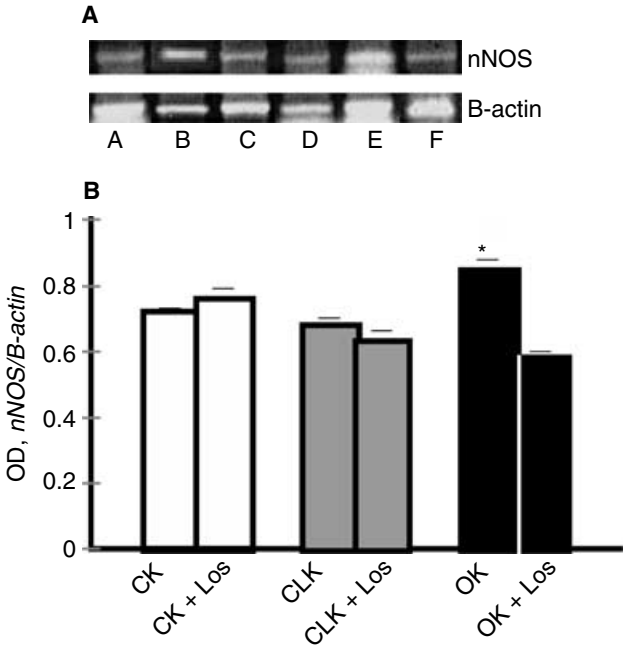

Fig. 5. Detection of neuronal nitric oxide synthase (nNOS) mRNA and β-actin gene by reverse transcription-polymerase chain reaction (RT-PCR) analysis in cortex of kidneys after unilateral ureteral obstruction (UUO). (A) Primers for nNOS (308 bp) were used in PCRs with cDNAs synthesized from the indicated tissues. The PCR products were analyzed on ethidium bromide–stained 1.5% agarose gels. Lane A, control cortex; lane C, contralateral cortex; and lane E, obstructed cortex. After treatment, lane B (control cortex) lane D (contralateral cortex), and lane F (obstructed cortex). Housekeeping gene β-actin expression is shown in the lower line in the same order as the densitometry bars. These results are one of six independent observations. (B) Semiquantitative PCR analysis of nNOS isoform in renal cortex of obstructed and control kidneys. Effect of AT_1 angiotensin II receptor antagonist, losartan (Los). In the vertical axis the ratio for nNOS/β-actin mRNA is shown. Increased nNOS/β-actin mRNA ratio in obstructed kidneys (OKs) ($N = 6$) related to control kidneys (CKs) ($N = 6$; $^*P < 0.05$) and to contralateral kidneys (CLKs) ($^{**}P < 0.01$). nNOS/β-actin mRNA ratio in renal cortex after losartan administration in obstructed kidney vs, nontreated obstructed kidneys ($N = 6$; $^{**}P < 0.01$). Values are means ± SEM.

and II) (Fig. 5). Decreased cortical nNOS expression was shown in obstructed kidneys after losartan administration 0.847 ± 0.03 vs. 0.589 ± 0.01 ($P < 0.01$). No changes on nNOS signals were observed on contralateral pretreated with losartan, nNOS 0.680 ± 0.020 vs. 0.630 ± 0.030 and on the control kidney cortexs after losartan, nNOS 0.720 ± 0.022 vs. 0.760 ± 0.030 (groups III and IV) (Fig. 5).

The amplified fragment of eNOS (325 bp) was observed in cortex of obstructed and contralateral kidneys,with less expression in control kidney cortex (Fig. 6B). Densitometric analysis of eNOS mRNA expresssion showed a significant increase in obstructed cortex related to control 1.30 ± 0.07 vs. 0.77 ± 0.03 ($P < 0.001$). Increase eNOS expression was observed in contralateral cortex vs. control cortex 1.60 ± 0.030 vs. 0.77 ± 0.03 ($P < 0.001$), lesser increased expression of eNOS was shown in contralateral kidney compared to obstructed kidney 1.60 ± 0.030 vs. 1.30 ± 0.07 ($P < 0.01$).

Treatment with losartan induced no changes in eNOS expression in obstructed cortex 1.30 ± 0.07 vs. 1.19 ± 0.02. No differences on eNOS expression were observed after losartan administration in control cortex and contralateral cortex 0.77 ± 0.03 vs. 0.81 ± 0.03 and 1.60 ± 0.07 vs. 1.57 ± 0.02, respectively (Fig. 6B).

TGF-β mRNA expression on renal cortex kidney in obstruction

We examined the expression of mRNA TGF-β in the obstructed kidney cortex. As shown in Figure 7, UUO induced an increased expression of TGF-β in obstructed kidneys compared to control kidneys and contralateral kidneys 0.839 ± 0.02 vs. 0.637 ± 0.03 ($P < 0.05$) and 0.839 ± 0.02 vs. 0.650 ± 0.02 ($P < 0.05$), respectively. Administration of losartan inhibited the induction of TGF-β, obstructed kidney 0.839 ± 0.02 vs. 0.666 ± 0.05 ($P < 0.05$). Losartan induced no differences on TGF-β expression in control and contralateral kidney cortexs 0.637 ± 0.03 vs. 0.625 ± 0.04 and 0.650 ± 0.02 vs. 0.670 ± 0.02, respectively (Fig. 7).

COX-2 protein expression

The relative amount of COX-2 protein was determined after normalization of the level of COX-2 protein of the control kidneys without treatment. Immunoblot analysis with an anti-COX-2 monoclonal antibody demonstrated slight enhance levels of COX-2 protein expression in obstructed cortex, 1.18 ± 0.04 ($P < 0.05$) and intensive increased protein expression in obstructed medulla 2.23 ± 0.03 ($P < 0.001$) relative to that in control kidneys. Increased COX-2 levels were observed in contralateral medulla relative to that of control medullas 2.22 ± 0.04 ($P < 0.001$).

On the contrary, down-regulation of COX-2 protein expression was demonstrated after losartan treatment in the obstructed cortex and obstructed medulla kidneys 0.83 ± 0.03 ($P < 0.01$) and 0.54 ± 0.04 ($P < 0.001$), respectively. Decreased COX-2 levels were observed in control medulla after losartan administration 0.50 ± 0.04 ($P < 0.01$).

COX-2 expression showed no differences on control cortex and contralateral kidney cortex and medulla, after losartan administration (Fig. 8).

Renal angiotensin II receptor binding

In kidneys, [^{125}I] Sar-1, Ile-8 angiotensin II binding was localized to the outer cortex and outer medullary regions. In the obstructed and control kidney cortex, the radioligand was localized in glomeruli, the subcapsular area, and in the longitudinal bands traversing the inner stripe

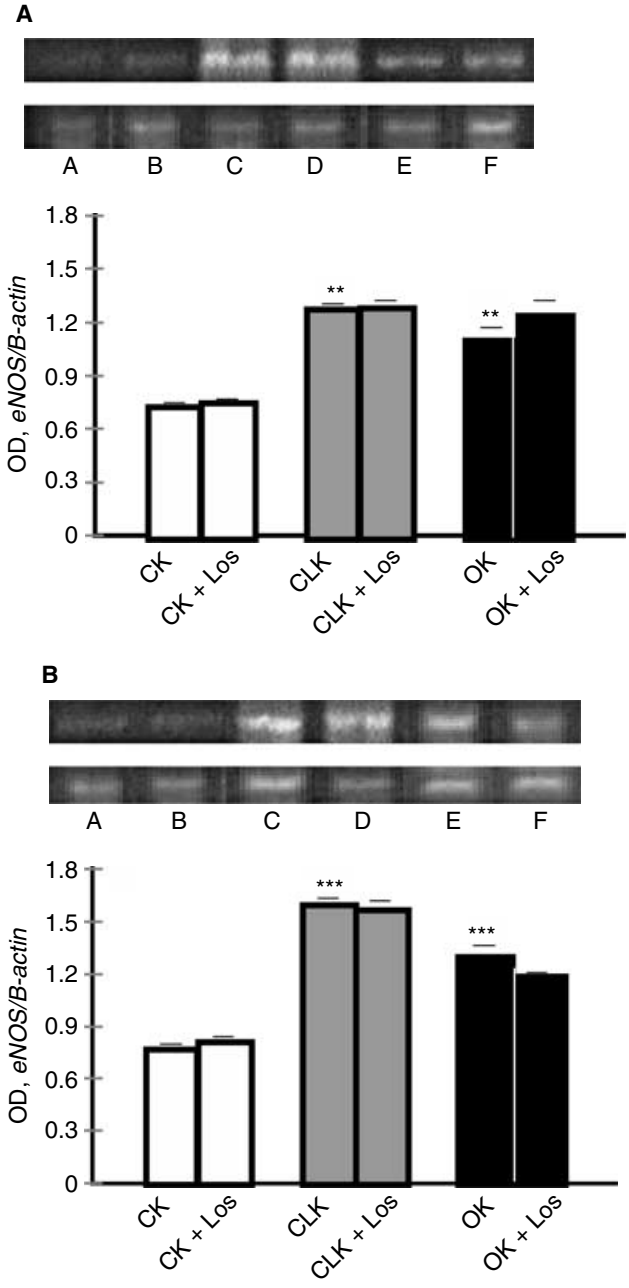

Fig. 6. Expression of endothelial nitric oxide synthase (eNOS) and β-actin mRNA in kidney medulla after unilateral ureteral obstruction (UUO). (*A*) Effect of losartan (Los). Polymerase chain reaction (PCR) products of control medulla (lane A), contralateral medulla (lane C), and obstructed medulla (lane E). After losartan treatment, lane B (control medulla), lane D (contralateral medulla), and lane F (obstructed medulla). Housekeeping gene β-actin expression is shown in the lower line, in the same order as the densitometry bars. These results are one of six independent observations. Semiquantitative PCR analysis of eNOS isoform in renal medulla. Graphic representation of eNOS/β-actin mRNA ratio shows increased expression in obstructed medulla vs. control medulla ($^{**}P < 0.01$). eNOS/β-actin mRNA ratio increase expression in contralateral medulla vs. control medulla was shown ($^{**}P < 0.01$). Values are means ± SEM. (*B*) Expression of eNOS and β-actin mRNA in kidney cortex after UUO. Effect of losartan. Primers for eNOS (325 bp) were used in PCRs with cDNAs synthesized from the indicated tissues. The PCR products were analyzed on ethidium bromide–stained 1.5% agarose gels. Lane A, control cortex; lane C, contralateral cortex; and lane E, obstructed cortex. After losartan treatment, lane B (control cortex), lane D (contralateral cortex), and lane F (obstructed cortex). The correspondying housekeeping β-actin is included in below the eNOS expression. These results are one of six independent observations. Semiquantitative PCR analysis of eNOS isoform in renal cortex. Graphic representation of eNOS/β-actin mRNA ratio shows increase expression in obstructed cortex vs. control cortex ($^{***}P < 0.001$). eNOS/β-actin mRNA ratio increase expression in contralateral cortex vs. obstructed cortex ($^{**}P < 0.01$) and in contralateral cortex vs control cortex ($^{***}P < 0.001$). Values are means ± SEM. Abbreviations are: CK, control kidney; CLK, contralateral kidney; OK, obstructed kidney.

of the outer medulla, corresponding to medullary vascular bundles and collecting ducts. Down-regulation of AT_1 receptors binding was shown in 24-hour unilateral obstructed kidneys (Fig. 9). Incubation of kidney slices in the presence of losartan markedly inhibited binding to the outer cortex and inner stripe of the outer medulla in obstruction leaving the sites corresponding to AT_2 receptor expression (Fig. 10). The densitometric analysis (Fig. 10) revealed a remarkable decrease of the binding to the AT_1 receptor in the cortex of obstructed kidneys, remaining only about 15% from the binding observed in the control kidneys. The same trend was observed in the inner stripe of the outer medulla. Decreased AT_1 receptor binding density was also observed in contralateral kidney, with a percentage of 30% from control. Minimal binding density of AT_1 receptors was detected in the papillary region of experimental and control kidney groups.

Intense decrease on AT_1 angiotensin II receptor binding was observed after losartan treatment (10 mg/kg, oral dose) in cortex and in inner stripe of the outer medulla in ipsilateral UUO related to control. No differences were observed in cortex and in inner stripe of the outer medulla in obstructed kidneys with losartan treatment compared to nontreated obstructed kidney group of animals. Lower AT_1 angiotensin II receptor binding was also shown in contralateral and control kidneys after oral losartan treatment.

Minimal binding to AT_2 receptor was shown to be constant in all groups studied and administration of losartan did not modify the number of AT_2 receptors in any case.

DISCUSSION

The study we present here adds to previous finding demonstrating that the AT_1 angiotensin II receptor inhibitor losartan is capable of blunting the progression of the fibrotic disease, improving renal architecture in obstruction. This effect, involving modulation of the expression of NOS isoforms and COX-2, is independent from changes in blood pressure.

Enhanced expression of renin-angiotensin system (RAS) genes, involved in the pathogenesis of interstitial fibrosis, has been demonstrated in UUO [5]. Intrarenal

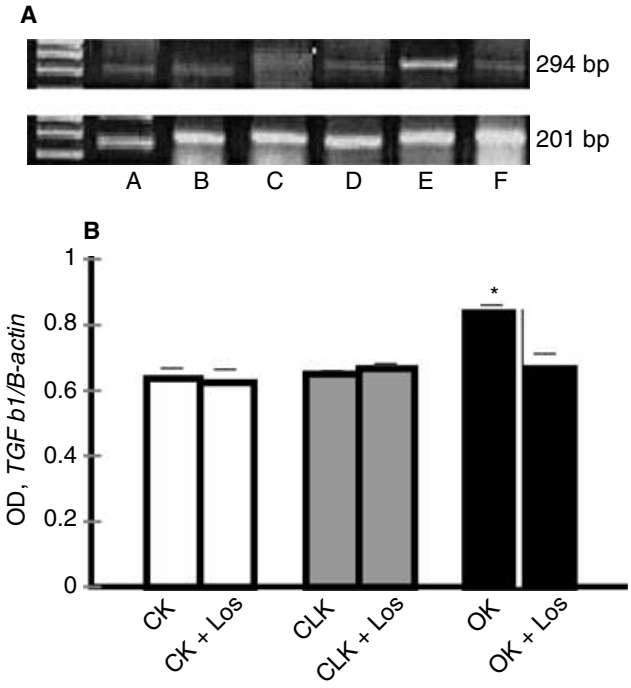

Fig. 7. Reverse transcription-polymerase chain reaction (RT-PCR) analysis of transforming growth factor-β (TGF-β) and β-actin mRNA in renal cortex, 24 hours after unilateral ureteral obstruction (UUO). (*A*) Effect of losartan (Los). Aliquots of cDNA prepared from cortex of obstructed (OK), contralateral (CLK), and control kidneys (CK) were coamplified for 30 cycles with TGF-β–specific primers (294 bp) and with β-actin–specific primers. The products were separated on 3% agarose gels and visualized by ethidium bromide staining. Lane A, control cortex; lane C, contralateral cortex; and lane E, obstructed cortex. After losartan treatment, lane B (control cortex), lane D (contralateral cortex), and lane F (obstructed cortex). Housekeeping β-actin expression was shown in the lower line, below the TGF-β expression. The first nonlettered lane represents the migration of 100 bp ladder of molecular weight standards from Promega (Madison, WI, USA). These results are one of five independent observations. (*B*) Semiquantitative PCR analysis of TGFβ In the vertical axis the ratios are shown for TGF-β/β-actin mRNA in renal cortex after losartan administration ($N = 6$; $^*P < 0.05$ nontreated obstructed kidneys vs. control kidneys; $^*P < 0.05$ nontreated obstructed kidneys vs contralateral kidneys; $^*P < 0.05$ nontreated obstructed kidneys vs. treated obstructed kidneys). Values are means ± SEM.

concentrations of angiotensin II increase rapidly after the onset of ureteral obstruction being an early event in the damage cascade that lead to the accumulation of ECM proteins and renal damage [31]. Most of the biologic effects of angiotensin II are transduced by the presence and distribution of AT_1 receptors. Accordingly, we showed marked down-regulation of AT_1 receptor binding in obstructed kidneys presumably as the result of the increased intrarenal angiotensin II production, representing the activation of a negative feedback loop response- as it has been previously reported [32]. Renal fibrogenesis initiation at a very early stage, 24 hours of ureteral obstruction, was demonstrated throughout the expanded interstitium with twofold increase of interstitial volume and increased expression of TGF-β within the affected kidney. Consistent with our results, a significant up-regulation of TGF-β and its type 1 receptor expression in the kidneys 1 day after obstruction have been reported in an earlier study [33]. TGF-β plays an essential role in initiating epithelial-mesenchyme transformation that leads to the accumulation of matrix-producing myofibroblast cells [34]. The profibrotic role of angiotensin II has been demonstrated by the induction of TGF-β type I and type II receptors and increased synthesis of TGF-β in fibroblasts, smooth muscle cells, and renal mesangial cells [35]. No tubular atrophy was demonstrated in obstructed kidneys. An increase in distal tubule compliance [36] and enhanced intraluminal hydrostatic pressure could explain the dilatation in obstructed medullary collecting duct segments we have demonstrated.

Administration of a nonhypotensive dose of the AT_1 angiotensin II receptor inhibitor losartan for 15 days before 24 hours of UUO in our study nearly produced protection against tubulointerstitial fibrosis with TGF-β mRNA expression in obstructed kidneys similar to controls. Evaluation of histologic indexes showed that losartan treatment significantly decreased the expansion of the interstitium in the obstructed kidney with no differences in the volume fraction (Vv) of the cortical intertitium between the obstructed kidney after losartan administration and control kidneys.

Increased nitric oxide generation has been shown to ameliorate interstitial fibrosis. Arginine, as a direct precursor to nitric oxide, and ACE inhibitors involved in the augmentation of nitric oxide production by stimulating bradykinin [37] have been found to blunt the fibrosis response in obstruction. Although the protective role of nitric oxide has been studied, results, including its molecular source, are still in conflict. Target deletion of the iNOS gene (iNOS−/−mice) have been demonstrated to exacerbate interstitial fibrosis [38]. On the contrary, results of Huang et al [39] have shown fibrosis reduction involving cNOS isoforms for its modulation in knockout iNOS mice. Inhibition of COX-2 reduces TGF-β expression, resulting in decreased tubular damage and interstitial fibrosis in obstruction. There is mounting evidence for a biologic relationship between prostanoid and nitric oxide biosynthesis. Continuous production of these molecules is involved in chronic inflammatory conditions [40]. Endogenous nitric oxide is necessary for sustained COX-2 expression and prostaglandin synthesis in macrophages [41].

In the present study, an intensive increase of iNOS activity and expression in obstructed renal medulla with lesser iNOS activity and expression on obstructed cortex were shown, as we have previously reported [42]. Early cellular events postobstruction, including renal interstitial macrophage infiltration and angiotensin II upregulation inducing increase on cytokine expression and activity, are involved in the iNOS isoform expression in

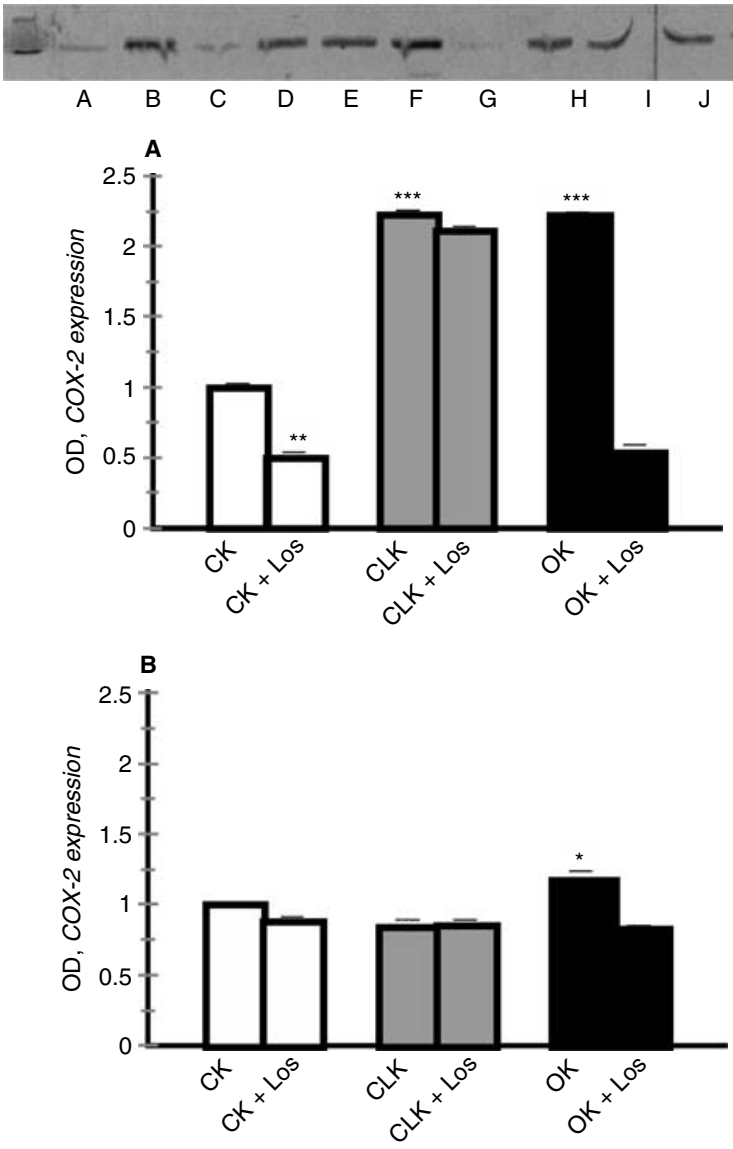

Fig. 8. Effect of losartan on renal cyclooxygenase-2 (COX-2) protein expression in vivo. Immunoblotting analysis of COX-2 from cortex and medulla of rats treated by losartan (10 mg/kg). Lanes A and B, Control medulla and cortex; lanes C and D, control medulla and cortex-losartan treated; lanes E and F, obstructed medulla and cortex; lanes G and H, obstructed medulla and cortex-losartan-treated; lanes I and J, contralateral medulla and cortex; lanes K and L, contralateral medulla and cortex-losartan treated. The first nonlettered lane represents the protein standart (COX-2, 72 kD). Densitometric analysis of COX-2 protein abundance in unilateral ureteral obstruction (UUO). Effect of losartan. Immunoblots were quantified for COX-2 expression. The relative amount of COX-2 protein was determined after normalization of the level of COX-2 protein of the appropriate control without treatment to 1. (*A*) Renal cortex. Nontreated obstructed kidneys (OKs) vs. control kidneys (CKs) ($^{*}P < 0.05$, nontreated obstructed kidneys vs. contralateral kidneys (CLK); $^{**}P < 0.01$, nontreated obstructed kidneys vs. treated obstructed kidneys). (*B*) Renal medulla of obstructed and control kidneys. Effect of losartan. Nontreated obstructed kidneys vs. control kidneys ($^{***}P < 0.001$, nontreated obstructed kidneys vs. treated obstructed kidneys; $^{**}P < 0.01$, control kidneys vs. treated control kidneys). Data represent mean ± SEM from five separate experiments.

obstruction [43, 44]. The lesser iNOS expression activity we have observed in the obstructed cortex could be presumably related to the increased expression of TGF-β and its role in inducing a negative modulation of the iNOS expression. TGF-β reduces iNOS expression by decreasing iNOS mRNA stability and iNOS mRNA translation, while increasing degradation of iNOS protein [45]. On the contrary, twofold increased cNOS activity accompanied by an increased eNOS and nNOS mRNA was demonstrated in obstructed renal cortex. Similar to our results in renal kidney cortex from angiotensin II–infused hypertensive rats, an experimental model of intrarenal angiotensin II, increased cNOS activity and nNOS and eNOS protein expression have been demonstrated [46].

The role of constitutive NOS mainly related to eNOS isoform in ameliorating interstitial fibrosis could be suggested due to our previous study [44] and from others showing a significant role of increased eNOS for downregulating renal fibrosis [39], and loss of eNOS contributing to increased tubulointerstitial renal injury [47].

Early proteinuric diabetic nephropathy increased eNOS renal expression with enhanced indices of renal oxidative/nitrosative stress. Angiotensin receptor blockers decreased both renal NADPH oxidase and eNOS, preventing the development of oxidative damage [48].

In our results of increased cNOS activity, enhanced nNOS isoform expression was demonstrated in obstruction. A role to nNOS as a marker of renal injury can be inferred through recent studies showing nNOS generation of reduced oxygen species, including superoxide O^{-}_{2} and hydrogen peroxide (H_2O_2), in the absence of L-arginine [49]. nNOS also exerts a counteracting modulatory influence on TGF-mediated afferent arteriolar constriction [50]. Selective increase in renal vascular

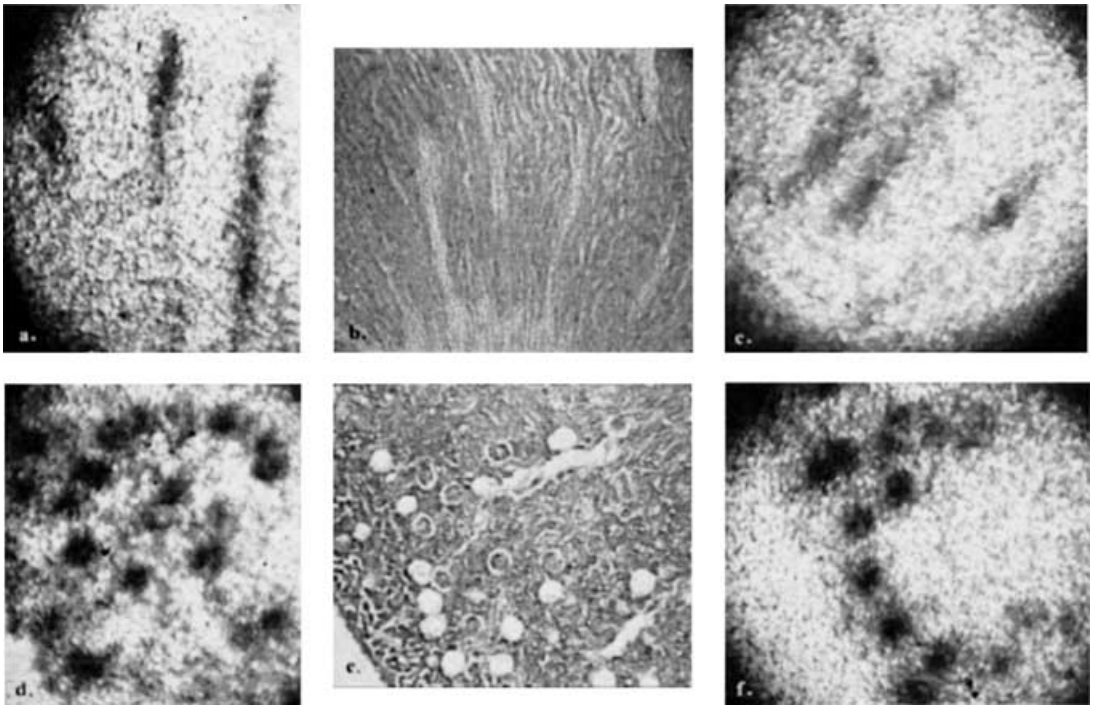

Fig. 9. Autoradiographic images of ^{125}I-Sar1-Ile8-Angiotensin II binding to regions of the obstructed and control kidneys. Binding in the control (*a*) and obstructed kidney (*c*) is located mainly to the longitudinal bands traversing the inner stripe of the outer medulla, corresponding to the medullary vascular bundles and collecting duct in the outer medulla of the kidneys and to the glomeruli in the renal cortex in control (*d*) and obstructed kidney (*f*). Histology of hematoxylin-eosin stained regions from obstructed kidney medulla (*b*) and obstructed kidney cortex (*e*) (magnification 78.7×).

resistance elicited by intrarenal angiotensin II levels have been demonstrated in obstruction.

The suggestion that macula densa nNOS regulates renin release and tubuloglomerular feedback by the activation of a second signaling system COX-2 has been reported [51]. Because of the localization of both nNOS and COX-2 in the cortical thick ascending limb of the loop of Henle (TALH), nNOS might be involved in mediating an increased COX-2 expression [52]. We have demonstrated high levels of COX-2 and nNOS expression, and these results allow us to suggest a close interaction between both, in modulating renal hemodynamics in obstructed cortex. In the present study, GFR was significantly reduced in obstructed kidney.Conversely, contralateral kidney GFR tended to be increased compared with the sham one. The abrupt and transient induction of RNA and protein products encoded by growth c-fos and c-myc genes, and later increased activity of related heat shock protein 70 (HSP70) and cH-ras genes, may possibly play a role in the initiation of the hypertrophic response, 24 hours following ureteral obstruction in contralateral kidney [53].

In our study, after an oral dose of losartan, no blood pressure–lowering effects were demonstrated; however, an intense anti-inflammatory action was evident due to the tubulointerstitial fibrosis protection. The intensive displacement of the iodinated tracer from its receptor demonstrated in cortex and inner stripe of the outer medulla in ipsilateral UUO showed no significantly decreased on AT_1 angiotensin II receptor binding after losartan treatment.

According with our results, recent observations have demonstrated that losartan elicits anti-inflammatory properties via its EXP3179 metabolite by blocking COX-2 -mRNA up-regulation, intracellular adhesion molecule (ICAM) mRNA regulation and cyclooxygenase-dependent thromboxane A_2 and prostaglandin F_2 generation in vitro independent of its blockade at the AT_1 receptor [54].

The in vivo effect of the AT_1 receptor antagonist losartan in our results showed decreased medulla iNOS mRNA and nNOS mRNA expression, persistent expression of eNOS in cortex, and decreased cortex and medulla COX-2 protein expression. These results allowed us to suggest a direct intrarenal anti-inflammatory leading to tubulointerstitial fibrosis protection throughout an independent action of losartan, involving NOS isoforms and COX-2, in obstruction.

The nonsuppressed angiotensin II levels, because of the increased ACE activity, despite a very low amount of renin mRNA, reported in contralateral related to control kidneys in unilateral obstruction [5] could probably explain the similar COX-2 protein levels in contralateral to obstructed kidneys. Medullary COX-2 protein

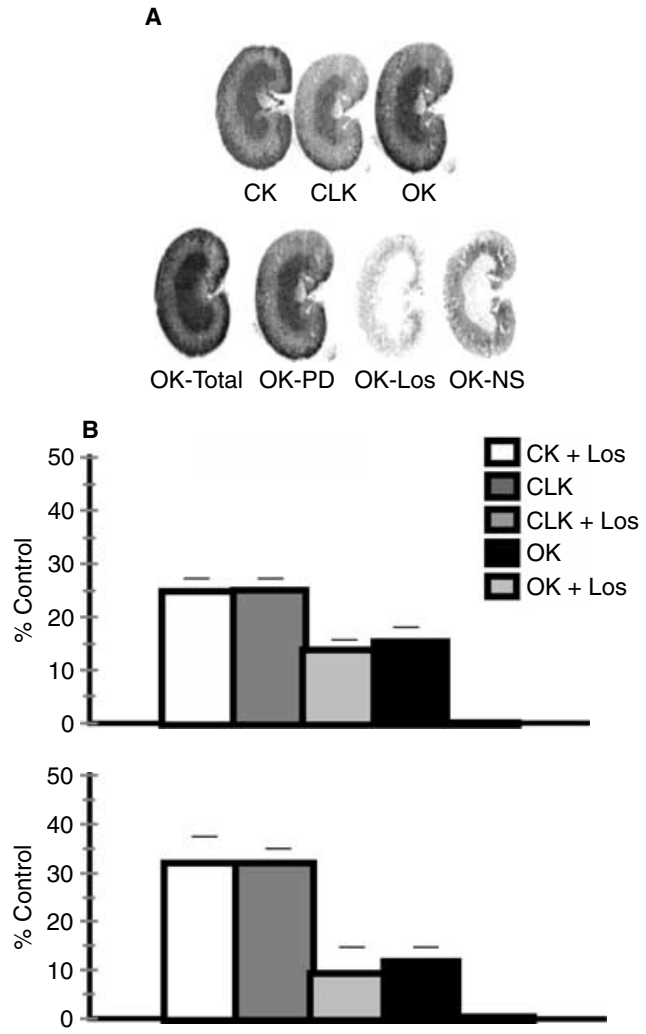

Fig. 10. Autoradiography and densitometiric measurements. (*A*) (Upper panel) Autoradiography of [^{125}I] Sar-1, Ile-8 angiotensin II binding 24 hours after unilateral ureteral obstruction (UUO). Control kidney (CK), contralateral kidney (CLK), and left obstructed kidney (OK) binding in presence of 1×10^{-5} mol/L PD123177 (AT_1 receptors). (Lower panel) In situ autoradiographic localization and identification of angiotensin II receptor subtypes in obstructed kidney after UUO for 24 hours. Longitudinal sections of rat kidney were incubated with [^{125}I] Sar-1, Ile-8 angiotensin II. Abbreviations are: OK-Total, angiotensin II binding occurred primarily in glomerular area and the inner stripe of outer medulla; OK-PD, incubation in the presence of PD123177 1×10^{-5} mol/L (AT_1 receptors); OK-Los, incubation in the presence of losartan 1×10^{-5} mol/L (AT_2 receptor expression) was markedly lower than AT_1 binding and confined to the glomerular and subcapsular area; OK-NS, nonspecific binding was defined by incubating kidney slices in the presence of 5×10^{-6} mol/L angiotensin II acetate. (*B*) Densitometric measurement of angiotensin II AT_1 receptor binding in UUO and control nontreated and losartan-treated kidneys. Binding to angiotensin II type 1 (AT_1) receptors, as determined by quantitative autoradiography, are expressed as a percentage from control kidneys. (Upper panel) Down-regulation of AT_1 receptor binding in obstructed renal cortex ($N = 5$) related to control. Decreased AT_1 receptor binding after losartan treatment. (Lower panel) Decreased AT_1 receptor binding in obstructed renal inner stripe of outer medulla ($N = 5$) related to control. As in cortex, decreased AT_1 receptor density after losartan. Kidney sections were incubated with [^{125}I]Sar^{1}Ile^8 angiotensin II (0.25 nmol/L) in the presence of 1×10^{-5} mol/L PD123319 to assess AT_1 receptors.

expression has been demonstrated to be restricted to interstitial cells, morphologically classified as fibroblasts and macrophages. The resident interstitial cells play a role in collagen production and interstitial fibrosis induction [55]. We have shown down-regulation of COX-2 protein expression in control medulla after losartan; involvement of its antifibrotic effect could infer, however, absence of morphometric changes were shown in controls.

Due to the increased inducible NOS activity in obstruction and to a previous support for a role of iNOS-generating nitric oxide and its interaction with superoxide for peroxynitrite, a potent oxidant [11], evidence for oxidative stress condition involved in the fibrotic process may be inferred in obstruction. Moreover, finding supporting the hypothesis that peroxynitrite is an important modulator of cyclooxygenase activity in inflammatory cells has been reported [56]. This mechanism provides an explanation for the enhancement of cellular prostaglandin biosynthesis by nitric oxide. While it has been assumed that $ONOO^-$ when nitric oxide generated from NOS reacts with exogenous O_2, it has been demonstrated that cellular nNOS and iNOS isoforms generate superoxide with secondary formation of $ONOO^-$ leading to cellular injury [49–57].

Our results of losartan down-regulation of iNOS, nNOS, and COX-2 with persistent levels of eNOS could suggest a profibrotic role of iNOS and nNOS isoforms in obstruction.

For the present results, we can conclude that at very early time obstruction, losartan protect for the fibrosis progression through out its anti-inflammatory effect, independent from changes on blood pressure. A modulation of NOS isoforms and COX-2 by AT_1 angiotensin II receptors could be included in the fibrosis blunted in obstruction. Our results underline the potential clinical implication of the fibrosis prevention in obstruction.

ACKNOWLEDGMENTS

The authors are grateful to Lic. Silvina Alvarez for assistance with COX-2 immunoblotting studies. This work was performed with financial support from the Research and Technology Council of Cuyo University (CIUNC) from Mendoza, Argentina/N: N:631/00 to P. Vallé.

Reprint requests to Walter Manucha, Ph.D., Cátedra de Fisiopatología, Facultad de Ciencias Médicas, Universidad Nacional de Cuyo, Centro Universitario CP 5500, Mendoza, Argentina.
E-mail: wmanucha@fmed2.uncu.edu.ar

REFERENCES

1. Eddy AA: Molecular insights into renal interstitial fibrosis. *J Am Soc Nephrol* 7:2495–2508, 1996
2. Remuzzi G, Bertani T: Pathophysiology of progressive nephropathies. *N Engl J Med* 339:1448–1456, 1998
3. Yang J, Liu Y: Delayed administration of hepatocyte growth factor reduces renal fibrosis in obstructive nephropathy. *Am J Physiol Renal Physiol* 284:F349–F357, 2003
4. Klahr S, Harris M, Purkenson ML: Effects of obstruction on renal function. *Pediatr Nephrol* 2:34–42, 1988

5. Pimentel JL, Martinez Maldonado M, Wilcox JN, *et al*: Regulation of renin-angiotensin system in unilateral ureteral obstruction. *Kidney Int* 44:390–400, 1993
6. Kaneto H, Morrissey J, Klahr S: Increased expression of TGF-β1 mRNA in the obstructed kidney of rats with unilateral ureteral ligation. *Kidney Int* 44:313–321, 1993
7. Kaneto H, Morrissey J, McCracken R, *et al*: Enalapril reduces collagen type IV synthesis and expansion of the interstitium in the obstructed rat kidney. *Kidney Int* 45:1637–1647, 1994
8. Ishidoya S, Morrissey J, McCracken R, *et al*: Angiotensin II receptor antagonist ameliorates renal tubulointerstitial fibrosis caused by unilateral ureteral obstruction. *Kidney Int* 47:1285–1294, 1995
9. Kaneto H, Morrissey J, McCracken R, *et al*: The expression of mRNA for tumor necrosis factor-α increases in the obstructed kidney of rats soon after unilateral ureteral ligation. *Nephrologie* 2:161–169, 1996
10. Mohaupt M, Schwobel J, Elzie JL, *et al*: Cytokines activate inducible nitric oxide synthase gene transcription in inner medullary collecting duct cells. *Am J Physiol* 268 (4 Pt 2):F770–F777, 1995
11. Pueyo ME, Arnal JF, Rami J, Michel JB: Angiotensin II stimulates the production of NO and peroxynitrite in endothelial cells. *Am J Physiol* 274 (*Cell Physiol* 43):C214–C220, 1998
12. Morrissey JJ, McCracken R, Kaneto H, *et al*: Location of an inducible nitric oxide synthase mRNA in the normal kidney. *Kidney Int* 45:998–1005, 1994
13. Nathan C, Xie Q: Regulation and biosynthesis of nitric oxide. *J Biol Chem* 269:13725–13728, 1992
14. Park CS, Park R, Krishna G: Constitutive expression and structural diversity of inducible isoform of nitric oxide synthase in human tissues. *Life Sci* 59:219–225, 1996
15. Salvemini D, Misko TP, Masferrer JL, *et al*: Nitric oxide activates ciclooxigenase enzymes. *Proc Natl Acad Sci USA* 90:7240–7244, 1993
16. Tetsuka T, Daphna-Iken D, Miller BW, *et al*: Nitric oxide amplifies interleukin 1-induced cyclooxygenase-2-expression in rat mesangial cells. *J Clin Invest* 97:2051–2056, 1996
17. Miyajina A, Chen J, Kirman I, *et al*: Interaction of nitric oxide and transforming growth factor-[beta] induced by angiotensin II and mechanical stretch in rat renal tubular epithelial cells. *J Urol* 164 (5):1729–1734, 2000
18. Perkins DJ, Kniss DA: Blockade of nitric oxide formation down-regulates cyclooxygenase-2 and decreases PGE_2 biosynthesis in macrophages. *J Leukoc Biol* 65:792–799, 1999
19. Timmermans PBMW, Ong PC, Chin AT, *et al*: Angiotensin II receptors and angiotensin II antagonists. *Pharmacol Rev* 45:205–251, 1993
20. Masson PJ: *J Techn Methods* 12:75–90, 1929 (AFIP modification)
21. Hruska KA, Guo G, Wozniak M, *et al*: Osteogenic protein-1 prevents renal fibrogenesis associated with ureteral obstruction. *Am J Physiol* (*Renal Physiol*) 279 F130–F143, 2000
22. Morrissey J, Hruska K, Guo G, *et al*: Bone morphometric protein-7 improves renal fibrosis and accelerates the return of renal function. *J Am Soc Nephrol* 13:S14–S21, 2002
23. Bredt DS, Synder SH: Nitric oxide mediates glutamate-linked enhancement of cGMP levels in the cerebellum. *Proc Natl Acad Sci USA* 86:9030–9033, 1989
24. Bradford MM: A rapid and sensitive method for the quantification of microgram quantities of protein utilizing the principle of protein-dye binding. *Anal Biochem* 72:248–254, 1976
25. Lyons CR, Orloff GJ, Cunningham JM: Molecular cloning and functional expression of an inducible nitric oxide synthase from a murine macrophage cell line. *J Biol Chem* 267:6370–6374, 1992
26. Bobadilla NA, Tapia E, Jimenez F, *et al*: Dexamethasone increases eNOS gene expression and prevents renal vasoconstriction induced by cyclosporin. *Am J Physiol* 277 (*Renal Physiol* 46):F464–F471, 1999
27. Fukuda K, Yoshitomi K, Yanagida T, *et al*: Quantification of TGF-β1 mRNA along rat nephron in obstructive nephropathy. *Am J Physiol Renal Physiology* 281:F513–F521, 2001
28. Viswanathan M, Tsutsumi K, Correa F, Saavedra J: Changes in the expression of angiotensin receptor subtypes in the rat aorta during development. *Biochem Biophys Res Commun* 179:1361–1367, 1991
29. Wang CS, Smith RL: Lowry determination of protein in the presence of Triton X-100. *Anal Biochem* 63:414–417, 1975
30. Gupta S, Srivastava M, Ahmad N, *et al*: Overexpression of cyclooxygenase-2 in human prostate adenocarcinoma. *Prostate* 42:73–78, 2000
31. Klahr S, Morrissey J: Angiotensin II and gene expression in the kidney. *Am J Kidney Dis* 31:171–176, 1998
32. Yoo KH, Norwood V, El-Dahr SS, *et al*: Regulation of angiotensin II AT_1 and AT_2 receptors in neonatal ureteral obstruction. *Am J Physiol* 273 (*Regulatory Integrative Comp Physiol* 42): R503–R509, 1997
33. Yang J, Liu Y: Blockage of tubular epithelial to myofibroblast transition by hepatocyte growth factor prevents renal interstitial fibrosis. *J Am Soc Nephrol* 13:96–107, 2002
34. Fan JM, Ng YY, Hill PA, *et al*: Transforming growth factor-beta regulates tubular epithelial-myofibroblast transdifferentiation in vitro. *Kidney Int* 56:1455–1467, 1999
35. Böttinger EP, Bitzer M: TGF-β signaling in renal disease *J Am Soc Nephrol* 13:2600–2610, 2002
36. Cortell S, Gennari FJ, Davidman M, *et al*: A definition of proximal and distal tubular compliance. Practical and theoretical implications. *J Clin Invest* 52:2330–2339, 1973
37. Morrissey J, Ishidoya S, McCracken R, Klahr S: Nitric oxide generation ameliorates the tubulointerstitial fibrosis of obstructive nephropathy. *J Am Soc Nephrol* 5:1585–1590, 1995
38. Hochberg D, Johnson CW, Chen J, *et al*: Interstitial fibrosis of unilateral ureteral obstruction is exacerbated in kidneys of mice lacking the gene for inducible nitric oxide synthase. *Lab Invest* 80:1721–1728, 2000
39. Huang A, Palmer Lane S, Hom D, *et al*: The role of nitric oxide in obstructive nephropathy. *J Urol* 163:1276–1281, 2000
40. Goodwind D, Landino L, Marnett LJ: Effects of nitric oxide and nitric oxide-derivates species on prostaglandin endoperoxide synthase and prostaglandin biosynthesis. *FASEB J* 13:1121–1136, 1999
41. Perkins DJ, Kniss DA: Blockade of nitric oxide formation down-regulates cyclooxygenase-2 and decreases PGE_2 biosynthesis in macrophages. *J Leukoc Biol* 65:792–799, 1999
42. Vallés PG, Manucha W: H^+-ATPase activity on unilateral ureteral obstruction: Interaction of endogenous nitric oxide and angiotensin II. *Kidney Int* 58:1641–1651, 2000
43. Klahr S, Morrissey J: The role of growth factors, cytokines, and vasoactive compounds in obstructive nephropathy. *Semin Nephrol* 18:622–632, 1998
44. Vallés PG, Pascual L, Manucha W, *et al*: Role of endogenous nitric oxide in unilateral ureteropelvic junction obstruction in children. *Kidney Int* 63:1104–1115, 2003
45. Vodovotz Y: Control of nitric oxide production by transforming growth factor β1: Mechanistic insights an potencial relevance to human disease. *Nitric Oxide* 1:3–17, 1997
46. Chin SY, Pandey KN, Shi SJ, *et al*: Increased activity and expression of Ca(2+) dependent NOS in renal cortex of ANG II-infused hypertensive rats. *Am J Physiol* 277 (5 Pt 2):F797–F804, 1999
47. Thomas SE, Anderson S, Gordon KL: Tubulointerstitial disease in aging: Evidence for underlying peritubular capillary damage, a potential role for renal ischemia. *J Am Soc Nephrol* 9:231–242, 1998
48. Onozato ML, Tojo A, Goto A, *et al*: Oxidative stress and nitric oxide synthase in rat diabetic nephropathy: Effects of ACEI and ARB. *Kidney Int* 61:186–194, 2002
49. Xia Y, Dawson VL, Dawson TM, *et al*: Nitric oxide synthase generates superoxide and nitric oxide in arginine depleted cells leading to peroxynitrite-mediated cellular injury. *Proc Natl Acad Sci USA* 93:6770–6774, 1996
50. Ito S, Johnson CS, Carretero O: Modulation of angiotensin II-induced vasoconstriction by endothelium-derivated relaxing factor in the isolated microperfused rabbit afferent arteriole. *J Clin Invest* 87:1656–166, 1991
51. Ichihara A, Navar G: Neuronal NOS contributes to biphasic autoregulatory response during enhances TGF activity. *Am J Physiol* 277 (*Renal Physiol* 46):F113–F120, 1999
52. Cheng HF, Wang JL, Zhang MZ, *et al*: Nitric oxide regulates renal cortical cyclooxygenase-2 expression. *Am J Physiol Renal Physiol* 278:F122–F129, 2000

53. Sawczuk IS, Hoke G, Olsson CA, *et al*: Gene expression in response to acute unilateral ureteral obstruction. *Kidney Int* 35:1315–1319, 1989
54. Krämer C, Sunkomat J, Witte J, *et al*: Angiotensin II receptor-independent antiinflammatory and antiaggregatory properties of Losartan. Role of the active metabolite EXP3179. *Circ Res* 90:770–776, 2002
55. Guan Y, Chang M, Cho W, *et al*: Clonning, expression, and regulation of rabbit cyclooxygenase-2 in renal medullary interstitial cells. *Am J Physiol* 273 (Renal Physiol 42):F18–F26, 1997
56. Landino LM, Crews BC, Timmons MD, *et al*: Peroxynitrite, the coupling product of nitric oxide and superoxide, activates prostaglandin biosynthesis. *Proc Natl Acad Sci* 93:15069–15074, 1996
57. Xia Y, Zweier JL: Superoxide and peroxynitrite generation from inducible nitric oxide synthase in macrophages. *Proc Natl Acad Sci USA* 94:6954–6958, 1997